

PRELIMINARY RESULTS OF THE ECHO-SEEDING EXPERIMENT ECHO-7 AT SLAC*

D. Xiang[†], E. Colby, Y. Ding, M. Dunning, J. Frederico, S. Gilevich, C. Hast, K. Jobe,
D. McCormick, J. Nelson, T.O. Raubenheimer, K. Soong, G. Stupakov, Z. Szalata,
D. Walz, S. Weathersby, M. Woodley, SLAC, Menlo Park, CA, USA
J. Corlett, J. Qiang, G. Penn, S. Prestemon, R. Schlueter, M. Venturini, W. Wan, LBNL, USA
P-L. Pernet, École Polytechnique Fédérale de Lausanne, Lausanne, Switzerland

Abstract

ECHO-7 is a proof-of-principle echo-enabled harmonic generation FEL experiment in the Next Linear Collider Test Accelerator (NLCTA) at SLAC. The experiment aims to generate coherent radiation at 318 nm and 227 nm, which are the 5th and 7th harmonic of the infrared seed laser. In this paper we present the preliminary results from the commissioning run of the completed experimental setup which started in April 2010.

INTRODUCTION

The remarkable up-frequency conversion efficiency of the echo-enabled harmonic generation (EEHG) technique [1, 2] has stimulated world-wide interests [3, 4, 5] in using EEHG to achieve fully coherent radiation in the x-ray wavelength from a UV seed laser. While significantly relaxing the requirements on laser power and beam slice energy spread as compared to the high-gain harmonic generation (HG) scheme [6], the EEHG requires more challenging control of the phase space correlations as the beam goes through the undulators and chicanes.

Two experiments to demonstrate the EEHG technique, one at NLCTA SLAC [7, 8] and the other at Shanghai DUV FEL [9], are now under commissioning. The echo-seeding experiment at SLAC (ECHO-7) is a generic EEHG proof-of-principle experiment that uses two different lasers (first laser has a wavelength of 795 nm and the other at 1590 nm) in the modulators. The experiment aims to generate the 5th and 7th harmonic of the second laser. Here we present the preliminary results from the commissioning run of the completed experimental setup which started in April 2010.

EXPERIMENT DESCRIPTION

The details of the ECHO-7 experiment are described in a separate paper of these proceedings [8]. The EEHG beam-line is schematically shown in Fig. 1. It consists of 3 chicanes (C0, C1, and C2) and 3 undulators (U1, U2 and U3). The mini-chicane (C0) is used to generate an orbit bump to allow laser injection into the first undulator (U1). The beam is modulated by the 795 nm laser in U1 and after passing through C1 separated energy bands will be generated. The beam is again modulated by 1590 nm laser in the second undulator (U2) and finally the separated energy

bands are converted to separated current bands after passage through C2. The density-modulated beam will produce coherent radiation in U3 which is presently tuned to 318 nm. The radiation generated in U3 is reflected by a downstream OTR screen to a UV-sensitive CCD which also measures the OTR from the screen itself.

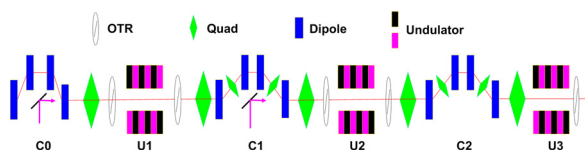


Figure 1: Schematic of the echo-seeding experiment

COMMISSIONING RESULTS

The experiment required installation of an additional X-band rf structure to boost the existing NLCTA 60 MeV beam to 120 MeV and the fabrication of the three chicanes and undulators. C0 was installed in October 2009 and C1 and C2 were installed in December 2009. A 75 cm long X-band rf structure, installed in December 2009, runs at a gradient of ~ 80 MV/m to boost the beam to 120 MeV. U1 and U2 were installed in February 2010 and the whole beam line was completed in April 2010 with the installation of U3. Now the experiment is under commissioning, with a staged goal to generate the 5th and 7th harmonic of the second laser.

With the new X-band structure we were able to measure the temporal profile of the electron bunch using the zero-phasing method. In the measurement, the beam is sent through the rf structure at the zero-crossing phase and then measured on a profile monitor downstream of the energy spectrometer. The horizontal beam size with the rf structure off is about $500 \mu\text{m}$ and the corresponding temporal resolution in the measurement is about 37 fs (the dispersion of the spectrometer is 46.5 cm). The results are shown in Fig. 2, from which one can see that the beam has a leading peak and a long tail. This is because the beam is on crest in the first x-band rf structure which accelerates the beam to 60 MeV and after passing through a pre-existing large chicane ($R_{56} = 74$ mm), located upstream of the second X-band structure, the head part of the beam is compressed while the tail part of the beam is decompressed.

The simulated bunch shape after the large chicane assuming a slice energy spread of 10 keV is also shown in the right plot of Fig. 2. While the general agreement is satisfactory, the width of the peak is about 2 times narrower in

* Work supported by US DOE contracts DE-AC02-76SF00515.

[†] dxiang@slac.stanford.edu

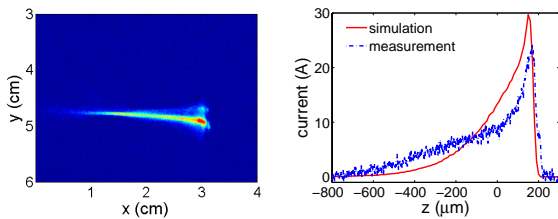


Figure 2: (Left) Measured beam profile after the spectrometer; (Right) Temporal profile of the beam.

experiment, which may indicate that the beam slice energy spread is at least a factor of 2 smaller than that used in the simulation.

In order to achieve beam-laser interaction, they need to overlap both spatially and temporally. The spatial overlap is achieved by steering the laser to the same position as the beam on the OTR screens upstream and downstream of the undulators. Some representative images measured on the OTR screens upstream and downstream of U1 are shown in Fig. 3. The laser size is about two times larger than that of the electron beam to provide uniform modulation in transverse direction. The beam image measured downstream of U1 consists of the contribution from both OTR and the undulator radiation (the 4 lobes are from the vertical component of the undulator radiation). The position jitters for the electron and lasers are on the order of a few tens of microns which is much smaller than the laser and electron beam size.

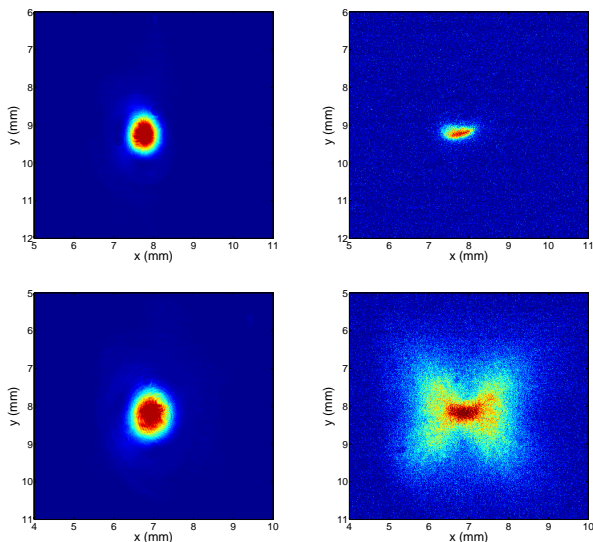


Figure 3: 795 nm laser image before (top-left) and after (bottom-left) U1; Electron beam image before (top-right) and after (bottom-right) U1.

In order to make the beam temporally overlap with the laser, the undulator radiation and the laser are first sent to a fast photodiode (300 ps rise time). By looking at the signal on a 2.5 GHz oscilloscope we were able to synchronize the laser and electron beam within 30 ps range. A delay stage is

then used to finely adjust the relative timing. The evidence of interaction between the laser and electron beam is observed by measuring the COTR signal on the OTR screen downstream of the chicane while scanning the laser time. Some representative results for the COTR signal vs laser timing are shown in Fig. 4. The enhancement of the COTR signal is only observed in a short time window in which the laser interacts with the beam. The FWHM of the time window of about $1 \sim 2$ ps depends on the electron bunch length, the laser pulse width and the timing jitter between the electron beam and the laser.

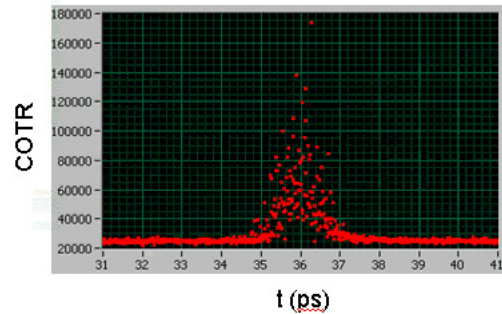


Figure 4: COTR intensity vs laser timing

The laser modulation amplitude is determined by scanning the laser energy with a wave plate while observing the COTR signal on the screen downstream of the chicane. The bunching factor for HGHG scheme is $b_n = J_n(nAB)e^{-n^2B^2/2}$, where n is the harmonic number, $A = \Delta E/\sigma_E$ is the dimensionless energy modulation amplitude and $B = R_{56}k\sigma_E/E$ is the dimensionless momentum compaction of the chicane. For a given R_{56} , one should see the oscillation of the COTR signal when scanning the laser energy. However, in our experiment the laser pulse width is comparable to the electron beam and there is a timing jitter of a few hundred fs between them, so the energy modulation amplitude varies along the beam. In the experiment, the measured COTR signal is the integrated signal for the whole bunch and it fluctuates from shot to shot, depending on the specific overlap of the laser and electron beam. For each wave plate angle, we recorded about 1000 interaction events and the resulting COTR peak intensity is shown in the left plot of Fig. 5. We also performed simulation using the measured beam longitudinal profile and the result is shown in the right plot of Fig. 5. A comparison between the simulation and measurement indicates that the peak energy modulation amplitude at maximum power for this laser is about 40 keV. This method is routinely used to set the laser power to provide the desired energy modulation.

After setting the delay stages to make the two lasers interact with the electron beam simultaneously, our first attempt in the EEHG experiment is to generate the 4th harmonic of the second laser. When both lasers are on, we observed a significant enhancement (more than one order of magnitude) of the signal at the exit of U3. The image recorded with a UV-sensitive CCD is shown in the left plot of Fig. 6. The coherent radiation is a combination of coher-

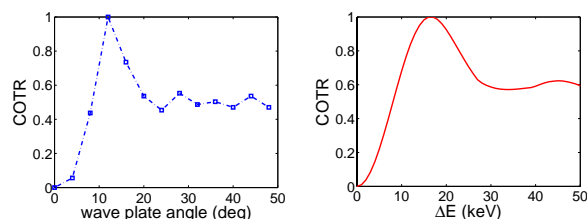


Figure 5: (a) Measured COTR peak intensity vs wave plate angle; (b) Simulated COTR peak intensity vs peak energy modulation amplitude.

ent undulator radiation and the COTR. The central bright spot consists of 795 nm COTR and 318 nm coherent undulator radiation. The inner bright ring is believed to be the off-axis undulator radiation at 398 nm while the outer rings are probably some reflection from the beam pipe. To confirm that there is radiation at the 4th harmonic of the 1590 nm laser, a 10 nm bandpass filter centered at 395 nm was put in front of the CCD camera and the result is shown in the right plot of Fig. 6. The ring shape of the radiation implies that it is the off-axis undulator radiation generated in U3. Note U3 only has 10 periods, so the radiation actually has a wide spectrum and there are plenty of off-axis photons at 398 nm generated in U3 at an angle of about 2.8 mrad.

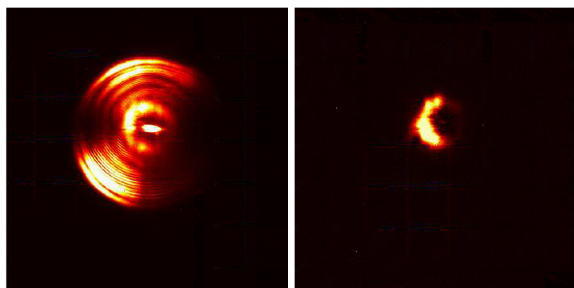


Figure 6: Radiation intensity on the OTR screen downstream of U3 with (right) and without (left) the bandpass filter.

DISCUSSION OF THE OBSERVATIONS

The observed signal at 398 nm could be generated by both the EEHG and the HGHG mechanisms. Due to the low slice energy spread of the beam, when either of the laser is turned off we still observed coherent radiation at 398 nm. While the intensity of the coherent radiation with both lasers is significantly higher than when only one laser is on, at present we can not unambiguously confirm that the signal is from EEHG.

First, there is still a possibility that the two lasers may interact with different parts of the beam. In our experiment the delay stage for each laser is set to make the COTR signal peak at the same laser timing so that the two lasers have the highest probability to interact with the same part of the beam. However, the beam timing jitter causes an uncer-

tainty of a few hundred fs in setting the laser timing. Second, the 1590 nm laser is shorter than the 795 nm laser. So there always exist some electrons that are only modulated by the 795 nm laser. These electrons could have a very small slice energy spread so that given a small energy modulation they could be effectively prebunched after passing through C1 and C2.

To resolve these issues and confirm the EEHG signal, we plan a number of upgrades to the NLCTA test facility. These include: 1) improved LLRF system to reduce the timing jitter, 2) optimization of the longitudinal bunch profile to reduce the bunch tails, 3) increase of the laser pulse lengths to increase the overlap with the beam, and 4) installation of a high resolution spectrometer and an rf deflector to resolve details of the longitudinal phase space.

CONCLUSIONS

A proof-of-principle EEHG experiment (ECHO-7) at SLAC has gone from the design stage into commissioning within one year. Significant enhancement of the radiation at the 4th harmonic of the second laser was observed when both lasers were interacting with the electron beam. While it is likely that the signal is from the EEHG technique, yet we can't preclude the possibility that the signal is from HGHG and more work is needed in order to unambiguously confirm the source of the signal.

ACKNOWLEDGEMENTS

We thank C. Adolphsen, J. Byrd, A. Chao, P. Emma, W. Fawley, J. Frisch, G. Hays, Z. Huang, H. Loos, H.-D. Nuhn, F. Wang, X. Wang, W. White, J. Wu and A. Zholents for helpful discussions, comments and commissioning assistances.

REFERENCES

- [1] G. Stupakov, Phys. Rev. Lett, 102 (2009) 074801.
- [2] D. Xiang and G. Stupakov, Phys. Rev. ST-AB, 12 (2009) 030702.
- [3] D. Xiang and G. Stupakov, "Coherent soft x-ray generation in the water window with the EEHG scheme", Proceedings of PAC'09.
- [4] E. Allaria, G. De Ninno and D. Xiang, "Feasibility studies for single stage echo-enabled harmonic in FERMI FEL-2", Proceedings of FEL09.
- [5] S. Reiche *et al.*, "Seeding option for the soft -xray beamline of SwissFEL", Proceedings of FEL09.
- [6] L.H. Yu, Phys. Rev. A, 44 (1991) 5178.
- [7] "Proposal for an echo-enabled harmonic generation experiment at NLCTA", SLAC LDRD programme, "<http://ldrd.slac.stanford.edu/2009%20Projects.asp>".
- [8] M. Dunning *et al.*, "A proof-of-principle echo-enabled harmonic generation experiment at SLAC", These proceedings, (2010).
- [9] J.H. Chen *et al.*, Proceedings of FEL09, (2009).